

Fatigue Tests of Two Prestressed Concrete I-Beams with Inclined Cracks

JOHN M. HANSON and C. L. HULSBOS

Respectively, Research Assistant Professor of Civil Engineering, and
Research Professor of Civil Engineering, Lehigh University

• AN IMPORTANT question in the design of prestressed bridge structures concerns the magnitude of overload to which the structure can be subjected without subsequently limiting the life of the bridge under design loads. The first step in the consideration of this question requires that the effect of the overload on the bridge structure, which manifests itself by the appearance of cracks in the main load-carrying members, be evaluated. The second step requires investigation of the fatigue properties of the cracked section under repeated loads.

Cracks in prestressed beams caused by applied loads may be of three types: flexural, flexure shear, or diagonal tension. Flexural cracks occur in regions of high moment and low shear, and propagate perpendicular to the longitudinal axis of the beam. Flexure shear and diagonal tension cracks are both inclined to the longitudinal axis of the beam. However, a flexure shear crack begins as a flexural crack and, because of the presence of shear, turns and becomes inclined in the direction of increasing moment. Diagonal tension cracks initiate from an interior point in the beam.

If a pretensioned prestressed beam subjected to an overload of sufficient magnitude to cause flexural cracking, without causing yielding of any of the prestressing elements, is subsequently subjected to similar repeated loads of equal or lesser magnitude, the number of repetitions of this load that the beam can endure before failure may be controlled by the fatigue strength of the concrete in compression or that of the prestressing strand in tension. Warner and Hulsbos (1) have shown that the fatigue life of under-reinforced beams will be controlled by the fatigue strength of the prestressing strand, and that stress repetitions smaller than the fatigue limit do not contribute to fatigue failure in the strand. Therefore, the overload will not cause failure if the beam is subsequently subjected to repeated loads which produce a stress in the strand less than the fatigue limit. Furthermore, in typical pretensioned prestressed beams which have been subjected to overloads great enough to cause flexural cracking, the stress level in the strand will reach the fatigue limit of the strand only under a moment substantially greater than that required to reopen the flexural cracks.

Next, in a pretensioned prestressed beam subjected to an overload of sufficient magnitude to cause inclined cracking, the fatigue life under lesser loads may again be controlled by either the concrete or the prestressing strand and, in addition, by the fatigue strength of the web reinforcement. The strain distribution in the region of the inclined cracking is nonlinear, and at the present time an analysis to determine accurately the stresses in the concrete, strand, and stirrups cannot be made. However, since inclined cracking occurs in regions of lesser moment, the stresses in the strand in this region are probably less critical than those in the region of maximum moment. Consequently, the critical component may be either the concrete or the web reinforcement. Research has shown that when deformed web reinforcement is crossed by diagonal tension inclined cracking, the stirrups in the region of the inclined crack yield immediately. Therefore, a pretensioned prestressed beam subjected to a single overload of sufficient magnitude to cause diagonal tension cracking may subsequently be critical in fatigue of the web reinforcement under lesser loads.

To explore the possibility of the type of failure discussed, two prestressed I-beams were subjected to a symmetrical two-point loading equal to 78 percent of the ultimate flexural capacity of the section. This loading was sufficient to cause diagonal tension cracking in both shear spans of both beams. Repeated loadings of lesser magnitude were then applied until failure occurred. Web reinforcement provided in the two test beams was 57 and 43 percent, respectively, of that required to develop the ultimate flexural capacity according to paragraph 1.13.13 of the AASHTO specifications (2). The two tests whose results are presented in this paper were part of a larger investigation (3, 4) of the ultimate strength of prestressed beams under the combined action of bending and shear, conducted by the Department of Civil Engineering at Fritz Engineering Laboratory, and sponsored by the Pennsylvania Department of Highways, U. S. Bureau of Public Roads, and the Reinforced Concrete Research Council.

NOTATION

- A = area of beam cross-section;
- c.g. = center of gravity of beam cross-section;
- c.g.s. = center of gravity of prestressing strand;
- E_c = modulus of elasticity of concrete;
- f'_c = ultimate compressive strength of concrete;
- f'_r = modulus of rupture of concrete;
- F = resultant force in prestressing strand;
- F_i = initial prestress force, before prestress release;
- I = moment of inertia of beam cross-section;
- N = number of cycles of repeated loading;
- Q = moment, about c.g., of area of cross-section on one side of horizontal section on which shearing stress is desired;
- r = percentage of web reinforcement, based on web width;
- R = stress interval;
- S = stress in strand, in percent of static ultimate tensile stress;
- S_{max} = maximum stress in repeated load cycle;
- S_{min} = minimum stress in repeated load cycle;
- V = applied load shear in test beams;
- V_c^f = applied load shear in test beams causing flexural cracking;
- V_c^{dt} = applied load shear in test beams causing diagonal tension cracking; and
- Z = section modulus.

TEST SPECIMENS

Description

The test beams, E.10 and E.11, were identical except for the web reinforcement. Details of the beams are shown in Figure 1.

Fabrication

The two beams were fabricated at the same time in a prestressing bed set up on the laboratory floor. The sequence of operations was as follows: tensioning the strands, positioning the web reinforcement, erecting the form, placing the concrete, curing, removing the form, instrumenting, and releasing the prestress.

Two 50-ton mechanical jacks were used to tension the straight strands. A special jacking arrangement was then used to adjust the tension in individual strands. The total prestress force at the time the concrete was placed, as measured by load cells placed on each strand, was 113.7 kips. The minimum and maximum prestress force in any individual strand was 18.7 and 19.1 kips, respectively.

Wire ties were used to secure the web reinforcement to the strand. Wood forms were used to cast the test beams. Checks made on the beams indicated that, in general,

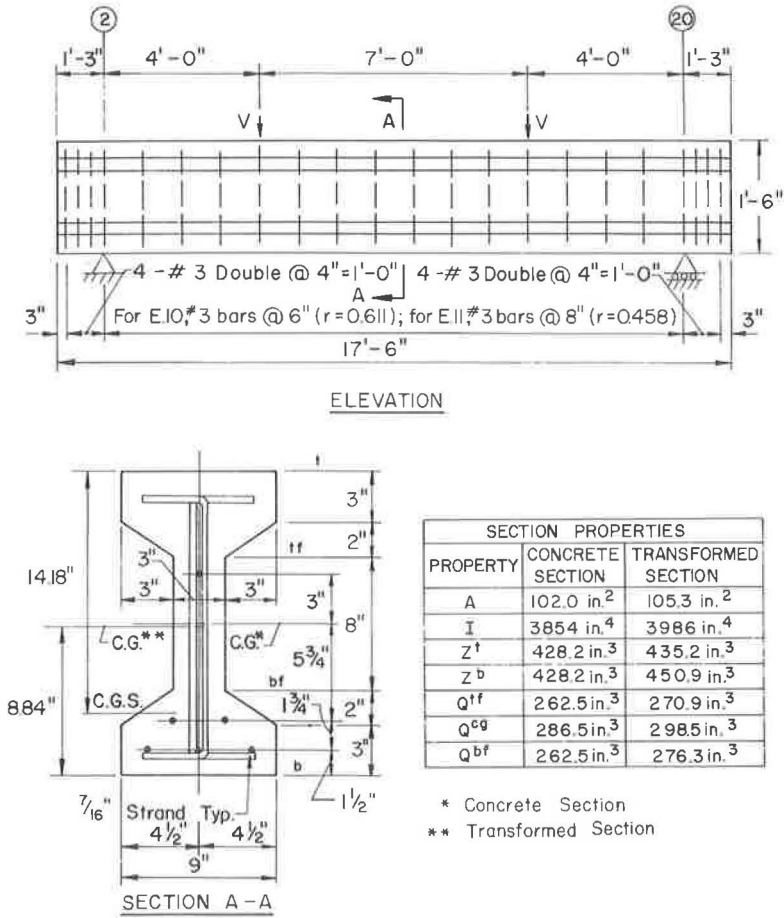


Figure 1. Details of test beams.

dimensions were maintained to within $\frac{1}{8}$ in., and consequently the nominal dimensions of the cross-section given in Figure 1 were used in all calculations. Cast simultaneously with each test beam were six 6- by 12-in. concrete cylinders and three 6- by 6- by 36- in. modulus of rupture specimens. Vibrators were used to place the concrete in both the test beams and the modulus of rupture specimens; the cylinders were rodded.

All specimens were covered with wet burlap and plastic sheeting for 5 days, after which the forms were removed. Instrumentation was positioned on the test beams on the sixth day. On the seventh day after casting, the prestress force was slowly released into the beams. The specimens were subsequently stored in the laboratory until tested.

Materials

Ready-mixed concrete, with a cement-to-sand-to-coarse aggregate ratio of approximately 1 to 1.8 to 2.3, was used to cast the test beams. The mix contained 7.5 sk/cu yd of Type III portland cement, and the maximum size of the coarse aggregate was $\frac{3}{4}$ in. The amount of water added to the mix produced a slump of 2.5 in.

A stress-strain curve for the $\frac{7}{16}$ -in. diameter seven-wire prestressing strand, determined from a tension test conducted in the laboratory, is shown in Figure 2. Failure occurred in the grips at an ultimate load of 26.3 kips. The stress-strain curve in Figure 2 was virtually identical with that provided by the manufacturer. According to

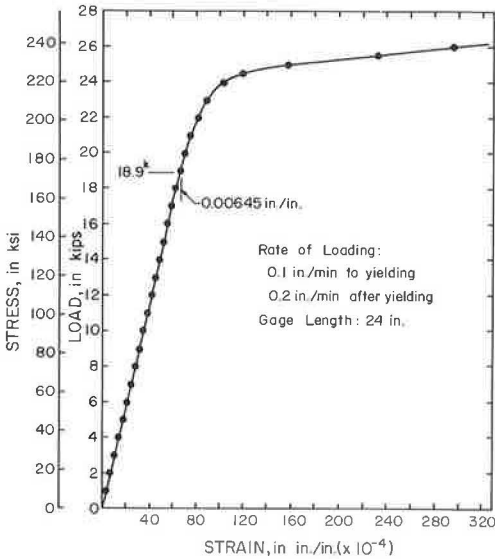


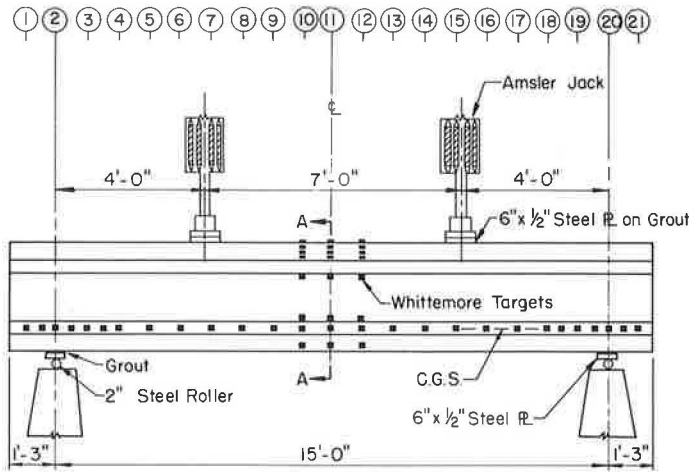
Figure 2. Stress-strain curve for pre-stressing strand.

the manufacturer, the ultimate load of the strand was 27.5 kips, corresponding to an ultimate stress of 252.2 ksi, and the elongation in 24 in. was 5.1 percent. The surface of the strand was free from rust, and care was taken to avoid getting any grease on the strand during fabrication.

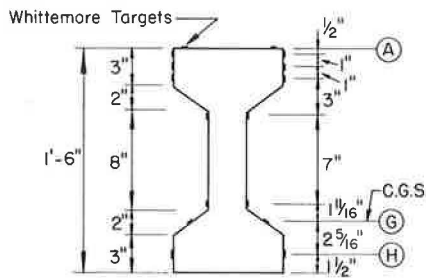
The web reinforcement was fabricated from hot-rolled No. 3 deformed bars, with a yield point of 55.5 ksi and an ultimate stress of 82.7 ksi, based on an area of 0.11 sq in.

Instrumentation and Loading Apparatus

The test setup and principal instrumentation employed on the test beams is indicated in Figure 3. Loads were applied symmetrically using two 55-kip Amsler hydraulic jacks bolted to a steel test frame. Vertical deflections were



ELEVATION



SECTION A-A

Figure 3. Test setup and principal instrumentation.

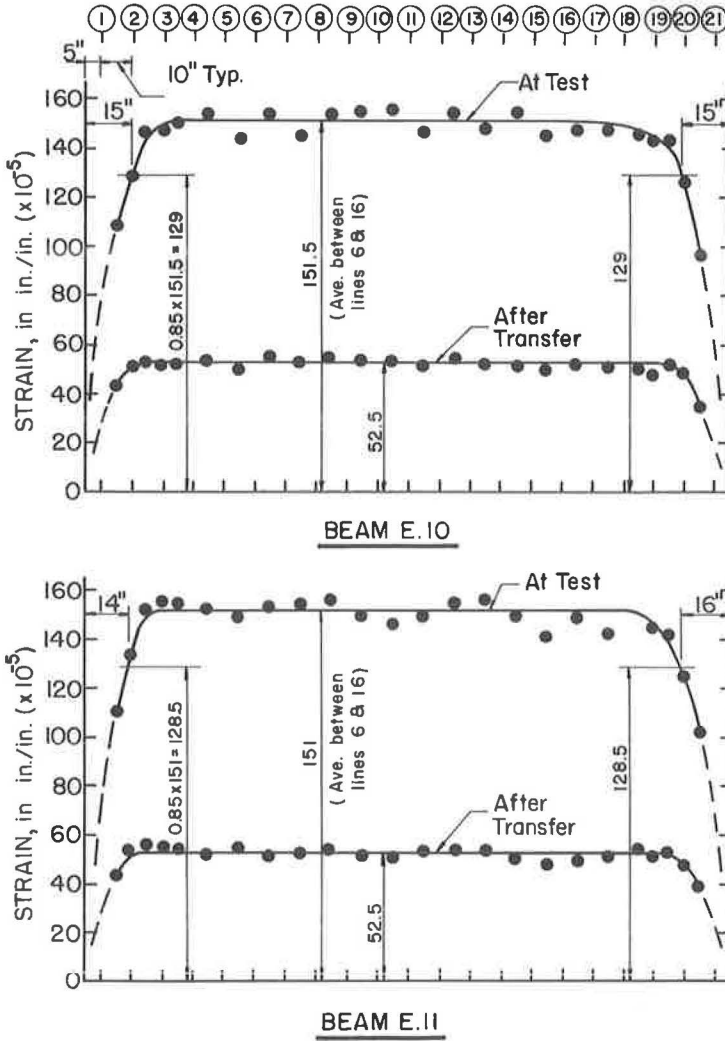


Figure 4. Concrete strain along c.g.s.

measured by Ames dial gages and level readings. Deformation data were taken using a 10-in. Whittemore strain gage. The Whittemore targets were cemented to the test beams with an epoxy resin. Crack widths were measured with a Gaertner 32 M/M EFL microscope with a built-in scale graduated to 0.001 in.

PROCEDURE AND RESULTS

Properties of Concrete

Compression tests were conducted on 6- by 12-in. cylinders to determine the ultimate compressive strength of the concrete, f'_c , associated with the test beams at prestress release and at test. Strains were measured on the cylinders with a compressor to determine the modulus of elasticity of the concrete, E_c . Modulus of rupture tests were conducted on plain concrete beam specimens having a 6- by 6-in. cross-section and loaded at the third points of a 30-in. span. The results of these tests and the age of the concrete at the time the test was conducted are given in Table 1. Each value of f'_c , f'_r , and E_c in Table 1 is an average of three tests.

TABLE 1
PROPERTIES OF CONCRETE

Beam	At Transfer			At Test			
	Age (days)	f'_c (psi)	E_c (ksi)	Age (days)	f'_c (psi)	f'_r (psi)	E_c (ksi)
E. 10	7	6,160	3,600	228	7,360	950	4,400
E. 11	7	6,410	3,600	245	7,790	960	4,200

TABLE 2
PRESTRESS DATA

Beam	Initial Prestress Force, F_i (kips)	Losses (%)		Prestress Force at Test, F (kips)	Transfer Distance (in.)	
		At Transfer	At Test		End 20	End 20
E. 10	113.7	8.4	23.7	86.7	15	15
E. 11	113.7	8.3	23.7	86.7	14	16

Prestress Data

Strain data were taken along line G shown in Figure 3 to determine the losses in the prestress force and the distance from the ends of the test beam at which 85 percent of the prestress force was effective, hereafter called the transfer distance. Readings were taken immediately before releasing the prestress force, immediately after release, and again just before testing. The differences between the first and second and between the first and third set of readings, converted to concrete strain, were plotted along the length of the test beam, as shown in Figure 4. The loss in the prestress force was determined, assuming that the concrete strain measured on the surface of the test beams at the c.g.s. was equal to the average strain loss in the prestressing strand. The transfer distance was determined from the plot of total concrete strain along the length of the test beam at the time of test, as shown in Figure 4. These results are presented in Table 2.

Loading History

The loading history for the two test beams is summarized in Table 3. Both test beams were first loaded statically, in increments of 1 or 2 kips shear, to a maximum applied load shear of 32 kips. The shears causing flexural cracking, V_c^f , and diagonal tension cracking, V_c^{dt} , during the first load cycle are given in Table 3.

Particular attention was given to the state of cracking in the shear spans at the time of formation of the diagonal tension cracks. Sketches of the crack patterns just after the formation of the diagonal tension cracks are shown in Figure 5. In these elevation views of E. 10 and E. 11, the solid heavy lines indicate all cracking before the formation of the diagonal tension cracks. The suddenly appearing diagonal tension cracks are indicated by dashed heavy lines. The location of the vertical stirrups are also shown by

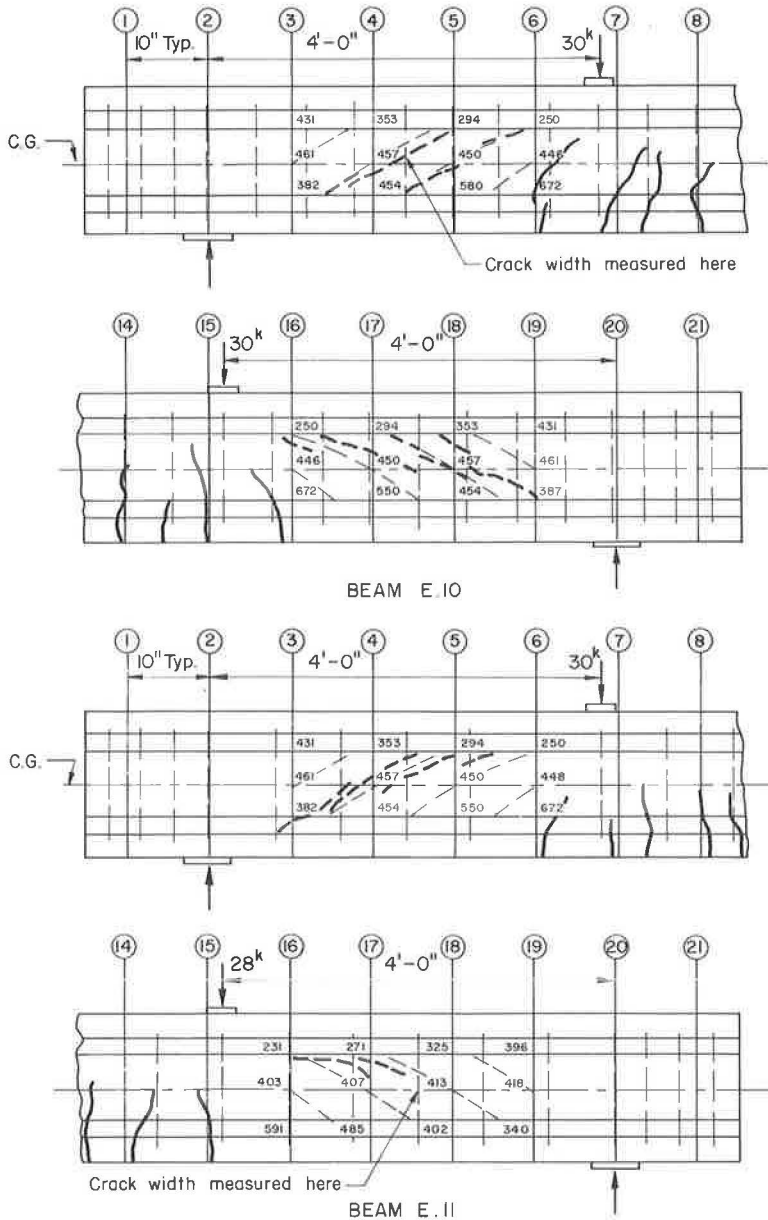


Figure 5. State of stress at diagonal tension cracking.

dashed light lines. Principal tensile stresses and the slopes of the compressive stress trajectories were calculated, using the properties of the transformed section, at the intersection of the grid lines within the shear span and the junction of the web and top flange, the mid-depth of the beam, and the junction of the web and bottom flange. It was assumed that the state of stress in the web was defined by a horizontal normal stress and a shearing stress and that the vertical normal stress was zero.

After being subjected to a maximum shear of 32 kips, the test beams were unloaded and subjected to several additional static tests to determine the load-deflection response of the cracked beam. In addition, Whittemore readings were taken during some of the static tests using primarily the group of targets on lines 10, 11, and 12. The width of

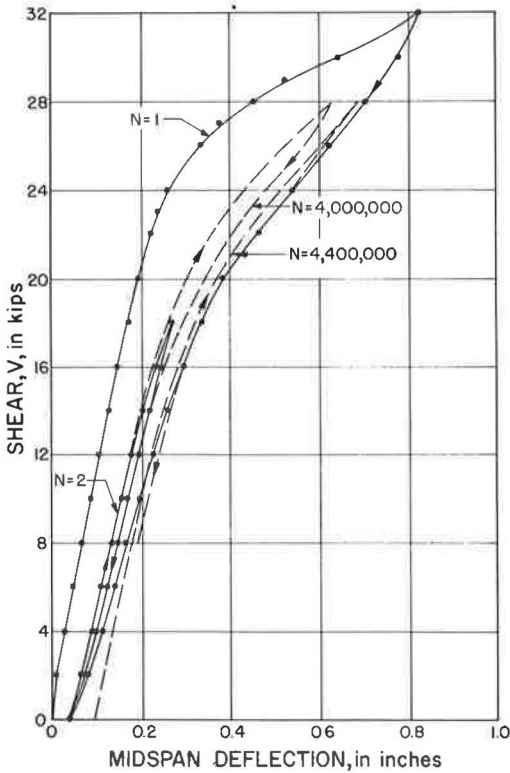


Figure 6. Load-deflection curve for E.10.

the diagonal tension cracks at the locations shown in Figure 5 was also measured.

The 0, 8 kip notation for V_{min} in Table 3 indicates that either of these values of shear correspond to the minimum load in the static load cycle. For example, in the case of E.10 beginning with the second load cycle, the load was varied from zero to a maximum of 18 kips and then back to zero. At this point, E.10 was permitted to rest overnight. Beginning with the third load cycle on the second day of the test, the load was taken from zero to 18 kips shear, and then back to 8 kips shear. The subsequent fourth through sixth static tests continued in the 8- to 18-kip range.

Similar static tests were conducted at selected intervals during the repeated loadings to take experimental readings. Rest periods, in general overnight, were permitted between static tests.

The repeated loading for both beams was applied at the rate of 250 cycles/min, except for the load cycles between 3,200,001 and 4,000,000 applied to E.10, when the loading rate was increased to 500 cycles/min. The magnitude of the maximum load applied in the repeated load cycle was controlled by the known load-

deflection response of the member determined from the preceding static tests; i. e., the magnitude of the repeated loading was adjusted so that the maximum deflection of the test beam while subjected to the repeated loadings was the same as the deflection in the static test at the corresponding load. The tests on E.10 and E.11 extend over 16 and 9 days, respectively.

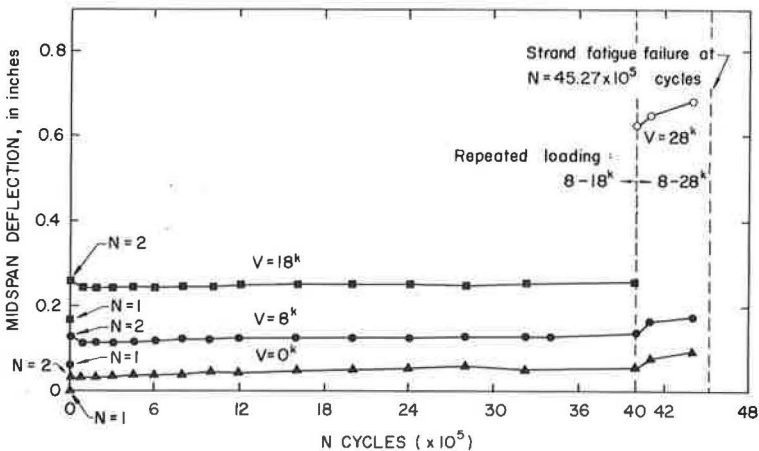


Figure 7. Deflection-N curves for E.10.

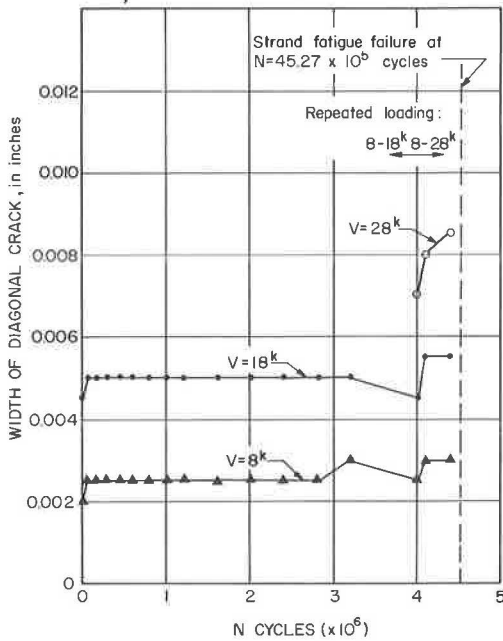


Figure 8. Variation in width of diagonal crack with N for E.10.

Behavior of E.10

As indicated in Table 3, the repeated loading applied to E.10 for the first 4,000,000 load cycles ranged from 8 to 18 kips shear. At N equal to 4,000,000 there was no indication of structural damage in the member; this prompted the decision to change the loading range to between 8 and 28 kips shear. Failure in E.10 occurred at N equal to 4,526,900 load cycles as a fatigue fracture in one wire of one of the bottom strands.

The load-deflection curve for E.10 at N equal to 1, 2, 4,000,000, and 4,400,000 is shown in Figure 6. Between N equal to 2 and N equal to 4,000,000 the load-deflection diagrams obtained from the static tests remained essentially unchanged. Between N equal to 4,000,000 and N equal to 4,400,000, the load-deflection diagram continually moved to the right. The load-deflection data obtained are summarized by the deflection- N diagram shown for E.10 in Figure 7, where corresponding to 0, 8, 18, and 28 kips

TABLE 3
LOADING HISTORY

Beam	Loading Cycle, N	V_{min} (kips)	V_{max} (kips)	Remarks
E.10	1	0	32	Initial static test: $V_c^f = 24$ kips $V_c^{dt} = 30$ kips, both ends.
	2-6	0, 8	18	Static tests.
	7-3, 200,000	8	18	Repeated load test at 250 cycles/min.
	3, 200,001-4, 000,000	8	18	Repeated load test at 500 cycles/min.
	4, 000,001-4, 526,900	8	28	Repeated load test at 250 cycles/min; fatigue failure in one wire of bottom strand at $N = 4, 526, 900$.
E.11	1	0	32	Initial static test: $V_c^f = 24$ kips $V_c^{dt} = 30$ kips, end 2, 28 kips, end 20.
	2-5	0, 8	24	Static tests.
	6-2, 007, 500	8	24	Repeated load test at 250 cycles/min; fatigue failure in stirrup, end 2, at $N = 2, 007, 500$.

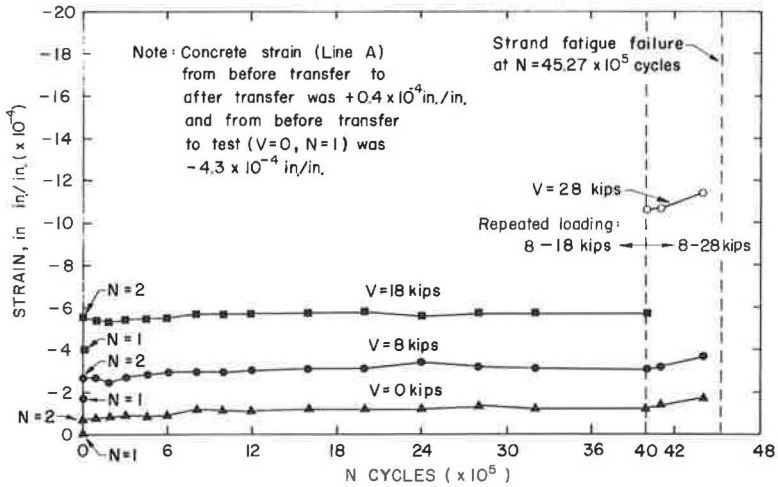


Figure 9. Variation in concrete strain of top fibers during test of E.10.

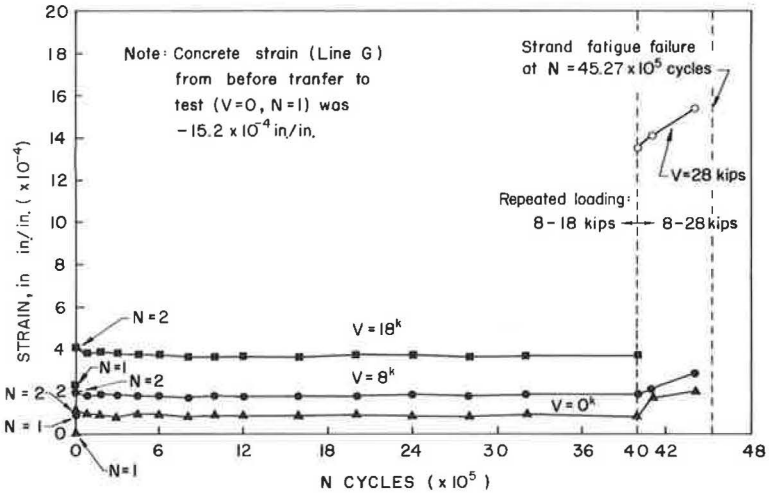


Figure 10. Variation in concrete strain at level of c.g.s. during test of E.10.

shear, midspan deflection is plotted against the N at which the static test was conducted.

After diagonal cracking in E.10, transverse crack width was measured at the location shown in Figure 5. At V equal to 30 kips, the crack width was 0.006 in. Increasing V to 32 kips opened the crack to 0.008 in. The width of the crack after the beam was unloaded was 0.002 in. Subsequent variation in the width of the crack at the minimum and maximum shear in the repeated load cycle with N is shown in Figure 8. In the static tests at any N, there was no observable opening of the crack up to a shear of 10 kips. From 10 kips to the maximum shear, the increase in crack width was approximately proportional to the increase in shear above 10 kips.

The Whittemore readings were used to determine the variation with N of the concrete strain in the top fibers (line A), at the c.g.s. (line G), and at the level of the lowest strand (line H) for the indicated values of shear, as shown in Figures 9, 10, and 11, respectively. Each point plotted in these figures is an average of four readings, i.e., an average of the readings between lines 10-11 and 11-12 on both sides of the member.

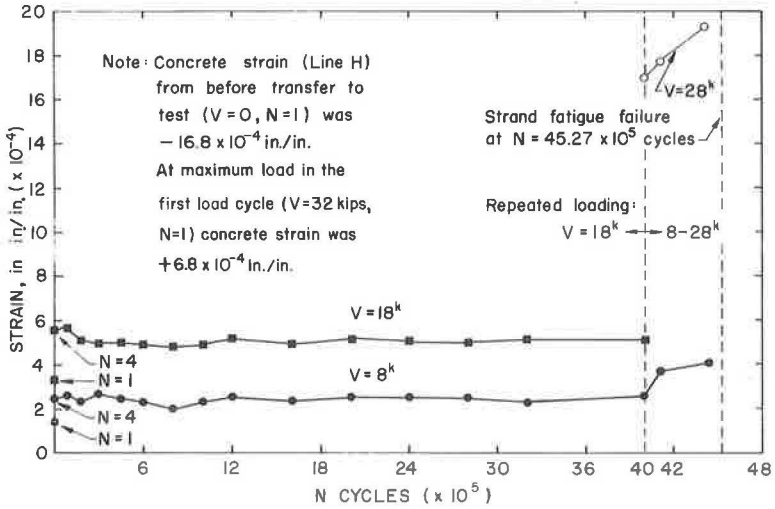


Figure 11. Variation in concrete strain at level of lower strand during test of E.10.

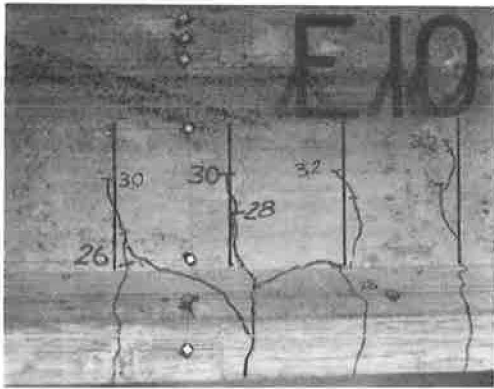


Figure 12. Strand fatigue failure region in E.10.

A closeup view of the failure region in E. 10 is shown in Figure 12. The vertical line of Whittemore targets is line 12. The failure was characterized by a sudden increase in the deflection of the test beam and a noticeable opening of the flexural crack in the region where the fatigue fracture of the strand occurred.

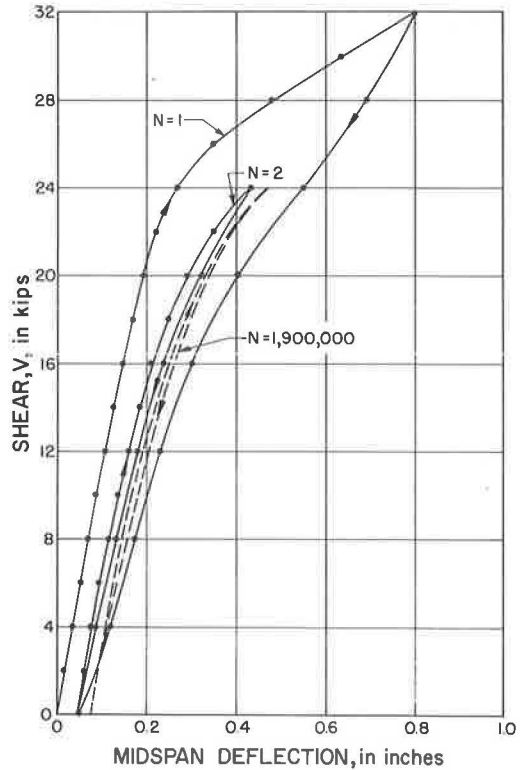


Figure 13. Load-deflection curve for E.11.

Behavior of E. 11

The repeated loading applied to E. 11 varied between 8 and 24 kips shear. Failure in E. 11 occurred at N equal to 2, 007, 500 load cycles as a fracture of the third stirrup from the support. An inspection of the failure region showed that the stirrup was not necked down at the fracture, and, therefore, the failure was considered to be a fatigue fracture.

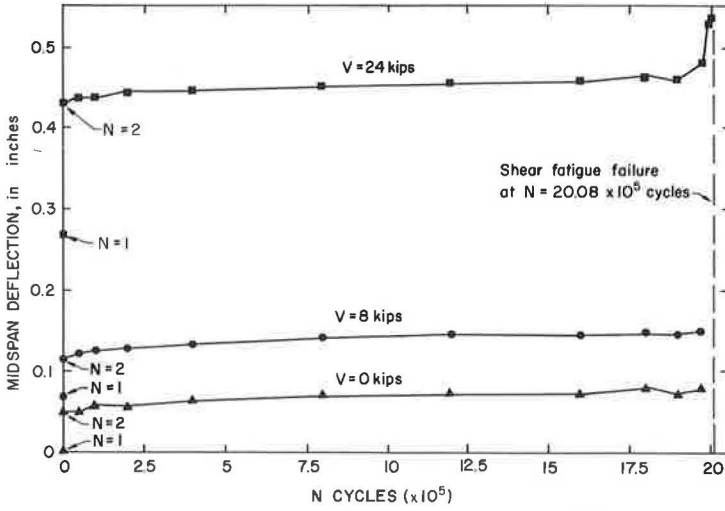


Figure 14. Deflection-N curves for E.11.

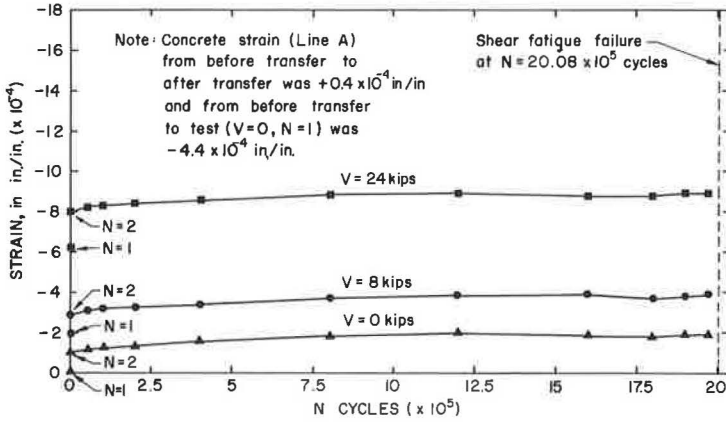


Figure 15. Variation in concrete strain of top fibers during test of E.11.

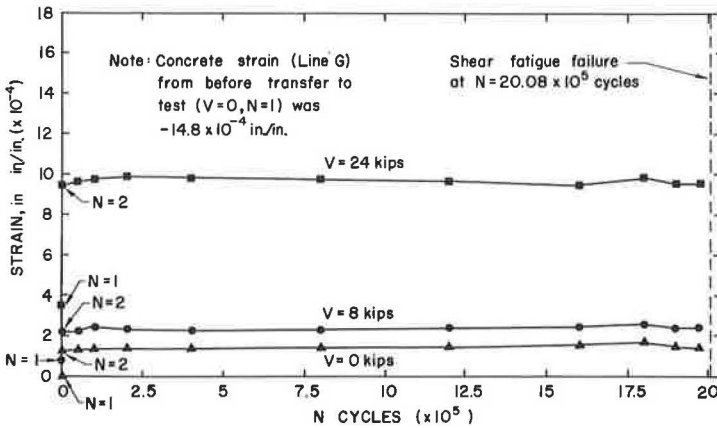


Figure 16. Variation in concrete strain at level of c.g.s. during test of E.11.

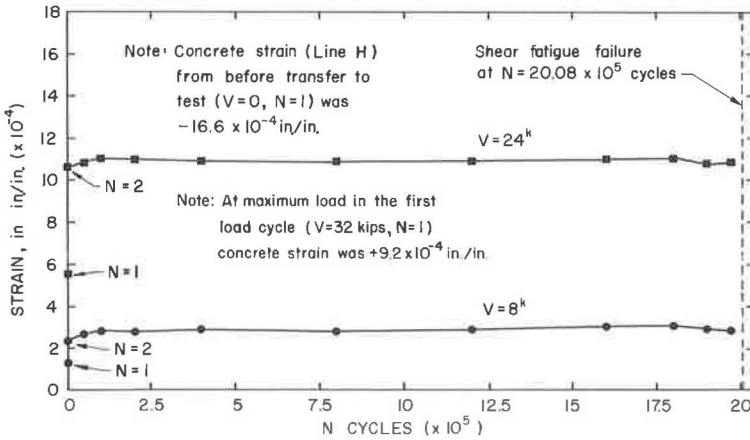


Figure 17. Variation in concrete strain at level of lower strand during test of E.11.

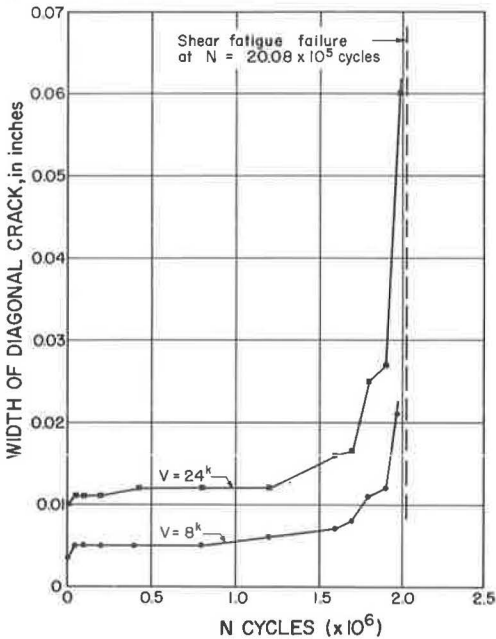


Figure 18. Variation in width of diagonal crack with N for E.11.

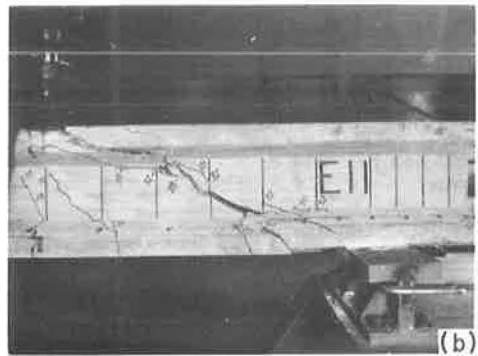
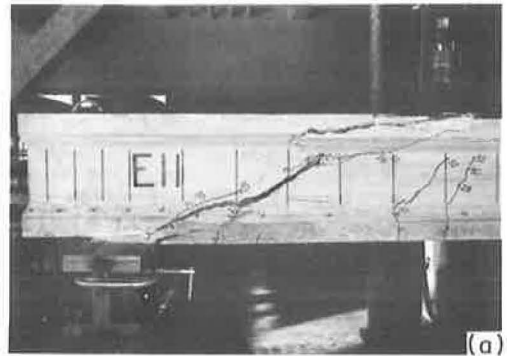


Figure 19. Shear fatigue failure region in E.11: (a) view of end 20; and (b) opposite side view of end 20.

Load-deflection curves for E. 11 at N equal to 1, 2, and 1,900,000 are shown in Figure 13. The deflection-N diagram shown in Figure 14 gives the variation in midspan deflection between N equal to 1 and 1,900,000 for values of shear equal to 0, 8, and 24 kips. Variation in concrete strain in the top fibers, at the c. g. s., and at the level of the lowest strand with N for the indicated values of shear is shown in Figures 15, 16 and 17, respectively.

The location shown in Figure 5 was selected to measure the transverse crack width after the crack had extended completely across the web at a shear of 30 kips. The width at V equal to 30 kips was 0.010 in. , and the crack opened an additional 0.001 in.

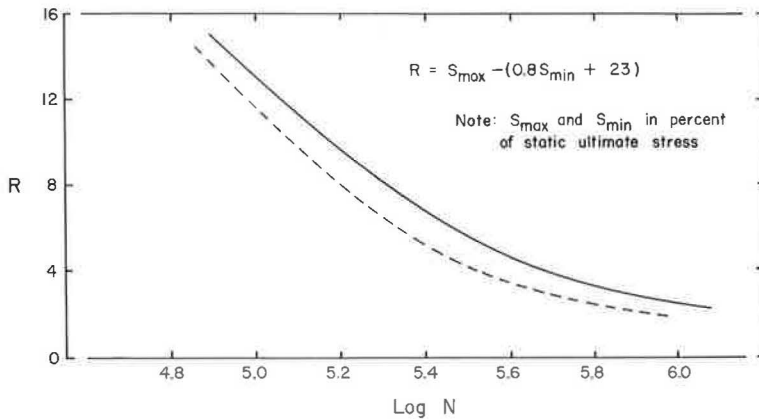


Figure 20. Fatigue properties of $\frac{7}{16}$ -in. diameter air furnace stress-relieved prestressing strand.

when the shear was increased to 32 kips. After the beam was unloaded, the crack had a residual width of 0.003 in. Subsequent variation in the width of the crack with N is shown in Figure 18. Again, there was no noticeable opening of the crack up to a shear of 10 kips, after which the increase in width was proportional to the increase in shear.

Closeup views of both sides of the failure region for E.11 are shown in Figure 19. The first visual evidence of structural damage was the noticeable increase in width of the diagonal crack, at approximately N equal to 1,500,000 cycles. Subsequently, noticeable extension of the diagonal cracking occurred, particularly in the region of the tension flange. The last static test was conducted at N equal to 1,970,000 cycles, at which time failure appeared imminent. However, the test beam was able to sustain an additional 77,500 load cycles. During this period, the diagonal crack continued to grow in width, until at failure the width was estimated as greater than $\frac{3}{16}$ in., wide enough to see completely through the web of the beam. The width of the crack appeared to increase at a nonuniform rate to be associated with extensions of the diagonal cracking. Final failure occurred suddenly when the diagonal tension crack extended through the compression flange. After the failure, it was observed that the third stirrup from the support was fractured.

DISCUSSION

The purpose of the tests on E.10 and E.11 was to determine if a prestressed beam subjected to an overload of sufficient magnitude to cause inclined diagonal tension cracking could subsequently be critical in fatigue of the web reinforcement under repeated loadings of linear magnitude. Identical counterparts of E.10 and E.11 (E.8 and E.9, respectively) have been statically tested by the authors (3, 4). These static tests were conducted on the same shear span to an effective depth ratio of 3.39 that was used for the repeated load tests on E.10 and E.11. Both E.8 and E.9 failed in flexure after the strand had yielded at the same ultimate moment of 167.7 kip-ft, including 2.9 kip-ft for dead-load moment. Therefore, the initial shear of 32 kips applied to E.10 and E.11 may be considered as an overload equal to 78 percent of their ultimate flexural capacity.

As indicated in Figure 11, the concrete strain in E.10 at the level of the lower strand was 0.168 percent compression from before transfer to test. The concrete strain at the same level caused by the application of the initial shear of 32 kips was 0.068 percent tension. Similarly for E.11, as indicated in Figure 17, the concrete strain from before transfer to test was 0.166 percent compression, and 0.092 percent tension due to the initial shear of 32 kips. Assuming that the concrete strain on the surface of the test beams at the level of the lower strand is equal to the change in strain in the strand, the strain in the lower strand at the 78 percent overload was still less than the initial prestressing strain of 0.645 percent. Therefore, no yielding of the strand occurred when the initial shear of 32 kips was applied to either E.10 or E.11.

After the initial overload, E.10 was subjected to 4,000,000 cycles of loading in which V ranged between 8 and 18 kips, corresponding to 21 and 45 percent of the ultimate flexural capacity of the beam. At V equal to 18 kips, the computed stress in the bottom fibers, assuming an uncracked section, was 210 psi tension. This loading range was regarded as representative of a typical bridge girder being repeatedly subjected to its design live load. However, after 4,000,000 cycles of this loading had been applied, there was no indication of structural damage in the member. Figures 7, 9, 10 and 11 show that there was no significant increase in deflection or change in strain in the constant moment region of the beam. Figure 8 shows that the width of the critical diagonal tension crack in the shear span had not increased and, furthermore, there had been no crack growth beyond that caused by the initial overload.

It was concluded that the 8- to 18-kip loading range was below the fatigue limit of the member and, therefore, the maximum shear in the loading range was increased to 28 kips. At V equal to 28 kips, E.10 was being subjected to a maximum moment equal to 69 percent of the ultimate flexural capacity, and the computed stress in the bottom fibers was 1,270 psi tension. Failure occurred after 526,900 cycles of this increased loading due to a fatigue fracture of one outer wire in one of the lower level strands. Figures 7 through 11 show that the deflection, crack width, and concrete strains had not stabilized during the period that this increased loading was applied. There is an indication, however, that this was due to creep, since these quantities were increasing at a decreasing rate and, therefore, were not an indication of the impending failure.

The fatigue fracture in E.10 was accompanied by a sudden increase in the deflection of the beam and a noticeable opening of the flexural crack in the region where the strand fracture occurred. The failure, however, was not catastrophic, and the beam could have carried, statically, a shear at least equal to the maximum shear of 28 kips applied in the repeated load cycle.

Following the initial overload to V equal to 32 kips, E.11 was subjected to a repeated loading which varied between 8 and 24 kips shear. At V equal to 24 kips, the maximum moment in the beam was equal to 59 percent of the ultimate flexural capacity, and the computed stress in the bottom fibers, assuming an uncracked section, was 810 psi tension. E.11 sustained 2,007,500 cycles of this loading before failure occurred.

Figures 14 through 17 show that the midspan deflection and the concrete strain in the constant moment region of E.11 remained nearly constant throughout the test, except for some slight effect of creep during the first part of the test. However, the increase in width of the critical diagonal crack, shown in Figure 18, after approximately 1,500,000 cycles is a definite indication of the impending failure in this region. The crack width was measured at the location where the fatigue fracture occurred. The increase in crack width was also associated with growth of the inclined cracking in the shear span, particularly in the later stages of the test.

The failure in E.11 occurred suddenly and would have been catastrophic under a gravity loading. The apparent cause of failure was the sudden extension of the inclined crack completely through the compression flange. It was subsequently determined that the third stirrup from the support had been fractured. However, it is quite possible that the fatigue fracture of the stirrup occurred before final failure, perhaps as early as N equal to 1,500,000 cycles.

The probable fatigue life of E.10 and E.11 may be determined, assuming that failure occurs at a fatigue fracture in the prestressing strand. The essential information required is the variation in stress with load in the most critically stressed strand, which for E.10 and E.11 is any one of the three lower strands. Since the Whittemore strain readings taken on line H are at the same level as the three lower strands, the assumption that the strain in the concrete is equal to the change in the strain in the strand from the initial prestressing strain permits the determination of the steel strain for any value of N directly from Figures 11 through 17.

Representative values of strain were selected at the minimum and maximum shear in the repeated load tests from Figures 11 and 17. These values were added algebraically to the initial strain of 0.645 percent and the strain from before transfer to test to give the strains in Table 4. The steel strains were converted to stress using the stress-strain curve for the strand in Figure 2.

TABLE 4
STRESS VARIATION IN LOWER LEVEL STRAND

Beam	Shear, V (kips)	Lower Level Strand		
		Strain (%)	Stress (ksi)	S (%) ^a
E. 10	8	0.500	133.0	52.6
	18	0.525	140.5	55.6
	28	0.645	173.5	68.6
E. 11	8	0.505	135.0	53.4
	24	0.585	157.5	62.3

^aOf static ultimate tensile stress of strand.

Warner and Hulsbos (1) have conducted an investigation of the fatigue properties of $\frac{7}{16}$ -in. diameter air furnace stress-relieved prestressing strand. The results of their tests are shown in Figure 20, where the solid line shows the relationship between the stress interval, R, and the mean fatigue life, N, of a single strand under constant cycle loading. The expected fatigue life of E. 10 or E. 11, however, would be less than the solid line because of the greater probability of failure in any one of the three lower level strands. This correction is indicated by the dashed line in Figure 20, which, therefore, represents the mean fatigue life of E. 10 or E. 11 assuming that a fatigue failure occurs in any of the lower level strand. For the 8- to 18-kip loading range on E. 10 and the 8- to 24-kip loading range on E. 11, R is negative, which indicates that the stress interval in the strand is below the fatigue limit. For the 8- to 28-kip loading range on E. 10, however, R is equal to 3.5 and, therefore, a strand fatigue failure would be expected after 4,000,000 cycles. E. 10 actually took 526,900 cycles of this loading range before failure occurred, which is good correlation.

The load-deflection curves for E. 10 and E. 11 in Figure 6 and 13, respectively, suggest a criterion for judging if fatigue may be critical in a prestressed beam with a diagonal tension crack. After cracking, the load-deflection response for E. 10 was essentially linear for V from 0 to 18 kips, but definitely nonlinear as the shear was increased to 28 kips. The load-deflection response for E. 11 was also nonlinear as V approached 24 kips. Therefore, in these tests the loadings which caused fatigue failures carried the beam into the nonlinear load-deflection range.

Finally, and perhaps most important, the results of the tests indicate that there are loadings for a prestressed beam which are more critical in fatigue of the web reinforcement than of the prestressing strand. Further testing is needed, particularly on different shear spans and with different amounts of web reinforcement, before the problem can be fully evaluated.

CONCLUSIONS

A prestressed beam subjected to an overload of sufficient magnitude to develop diagonal tension inclined cracking may be more critical in fatigue of the web reinforcement than in fatigue of the longitudinal prestressing strand. However, the two tests on a shear span-to-effective depth ratio of 3.39 reported here indicate that, in beams with approximately one-half of the web reinforcement required by paragraph 1.13.13 of the AASHTO specifications (2), an overload causing diagonal tension cracking will not cause a fatigue failure in the web reinforcement under design loads. A criterion for determining if the member is critical in fatigue after inclined cracking is the linearity of the load-deflection curve. That is, if the repeated loadings are within the range which permits the deflection of the member to remain essentially linear, the probability of a fatigue failure within the normal life of the member is small.

REFERENCES

1. Warner, R. F., and Hulsbos, C. L. Probable Fatigue Life of Prestressed Concrete Flexural Members. Lehigh Univ., Fritz Eng. Lab. Rept. No. 223.24A, July 1962.
2. Standard Specifications for Highway Bridges. 8th Ed. AASHTO, Washington, D. C., 1961.
3. Hanson, J. M., and Hulsbos, C. L. Overload Behavior of Prestressed Concrete Beams with Web Reinforcement. Lehigh Univ., Fritz. Eng. Lab. Rept. No. 223.25, Feb. 1963.
4. Hanson, J. M., and Hulsbos, C. L. Overload Behavior of Pretensioned Prestressed Concrete I-Beams with Web Reinforcement. Highway Research Record No. 76, pp. 1-31, 1965.